Pergamon

Mechanics Research Communications, Vol. 24, No. 1, pp. 41–47, 1997

0093-6413/97 $17.00 + .00

PII S0093-6413(96)00076-6

TRANSIENT NON-NEWTONIAN FLOW OF A SUSPENSION WITH A COMPRESSIBLE PARTICLE PHASE

Ali J. Chamkha, Department of Mechanical Engineering, Kuwait University, Safat, 13060 Kuwait

Abstract. Equations governing transient two-phase fluid-particle laminar flow over an infinite porous flat plate are developed. Both phases are assumed to behave as non-Newtonian power-law fluids. The mathematical model accounts for particle-phase viscous and diffusive effects. The particles are assumed spherical in shape and having a non-uniform density distribution. The resulting governing equations are nondimensionalized and solved numerically subject to appropriate initial and boundary conditions using an iterative, implicit, tri-diagonal finite-difference method. Graphical results for the displacement thicknesses and the skin-friction coefficients for both the fluid and particle phases are presented and discussed to illustrate special trends of the solutions.

(Received 2 October 1995; accepted for print 15 October 1996)

Introduction

The present work deals with unsteady laminar flow of a two-phase particulate suspension exhibiting a power-law non-Newtonian behavior over an infinite porous flat plate with suction being imposed at the surface. This problem is of interest due to its possible application in many industries such as the paint, pharmaceutical, and filtration industries. In addition, its governing equations reduce to ordinary differential equations whose solution exhibits a boundary-layer type behavior. In spite of theoretical and experimental evidence which show that a majority of particulate suspensions occurring in industries exhibit a non-Newtonian behavior (see, for instance Soo [1]), most continuum two-phase studies assume that the suspension is Newtonian in nature. The present paper treats both the carrier fluid and the particles as having nonlinear power-law stress-strain rate relationships.

The original dusty-gas model (meant to represent particulate suspensions having small particle volume fraction) discussed by Marble [2] has been used extensively in modeling two-phase particulate suspension flows. A generalized form of this model accounting for particle-phase stresses, particulate diffusion, and non-Newtonian effects as suggested by Soo [1], Peddieson [3], Ramshaw [4], Fredrickson [5], and Kapur [6] is reported. Thus, physical collection mechanisms such as inertial impaction and Brownian diffusion in non-Newtonian suspensions can be predicted. Kapur [6] reported closed-form solutions for a power-law fluid flow past an infinite flat plate with uniform suction. Chamkha and Peddieson [7,8] reported some approximate analytical and numerical results for the steady and transient Newtonian version of the present problem. Recently, Chamkha [9] reported numerical results for the steady version of the titled problem. This work represents an extension of the work by Chamkha [9]. While most of non-Newtonian fluids are highly thermodependent (i.e. their physical properties depend upon temperature, especially, their consistency index), all physical properties will be assumed constants herein as a first approximation. The particle phase is assumed to consist of non-deformable solids of spherical shape and have non-uniform density distribution.

Governing Equations

Consider transient flow of a power-law non-Newtonian particulate suspension past an infinite porous flat plate. Let the plate be placed along the x-axis corresponding to the plane $y=0$ and let the y-axis be normal to the flow direction. Let uniform fluid-phase suction be imposed at the plate surface with a velocity V_w. The flow is assumed laminar with fluid phase being incompressible and the particle phase being compressible.

The governing equations for this investigation are based on the balance laws of mass and linear momentum for the fluid and the particle phases. For the present problem, these equations reduce to (see, Chamkha and Peddieson [7] and Fredrickson [5]):

$$\partial_t\rho_p+\partial_y(\rho_p v_p)=0,\ \ \partial_t u-k\partial_y((\partial_y u)^m)-V_w\partial_y u+(N\rho_p)/\rho(u-u_p)=0,\ \ \partial_y P-N(D\partial_y\rho_p+\rho_p(v_p-V_w))=0$$

$$\rho_p\partial_t u_p-2^{(n-1)/2}k_p\partial_y(\rho_p\partial_y u_p(1/2(\partial_y u_p)^2+(\partial_y v_p)^2)^{(n-1)/2})+\rho_p v_p\partial_y u_p-N\rho_p(u-u_p)=0 \qquad (1)$$

$$\rho_p\partial_t v_p-2^{(n+1)/2}k_p\partial_y(\rho_p\partial_y v_p(1/2(\partial_y u_p)^2+(\partial_y v_p)^2)^{(n-1)/2})+\rho_p v_p\partial_y v_p+N(D\partial_y\rho_p+\rho_p(v_p+V_w))=0$$

where t is time and y is the normal distance above the plate. ρ, u, k, and P are the fluid-phase density, velocity in the x direction, phenomenological constant, and pressure, respectively. ρ_p, u_p, v_p, k_p are the particle-phase in-suspension density, velocity in the x direction, velocity in the y direction, and phenomenological constant, respectively. m and n are the fluid and particle behavior coefficient, respectively. N is an interphase force coefficient, and D is a diffusion coefficient. It should be noted that since the particle phase is assumed compressible, the particle phase exhibits a normal velocity gradient which contributes to extra terms in the particle-phase momentum equations. These terms increase the nonlinear coupling between the equations. It is also seen that the hydrodynamic interaction between the phases is restricted to a mutual linear drag force. In the present work N and D will both be treated as constants.

If both k_p and D are formally equated to zero, and m and n are equated to unity in Equations (1), the transient dusty-gas equations discussed by Marble [2] will be recovered. Also, if m and n are both set equal to unity and the particle-phase accelerations and stresses neglected in Equations (1), the usual convection Fickian diffusion with body forces will be recovered.

Since the plate is assumed infinite in length, all physical variables will only depend on t and y. Equations (1) can be made dimensionless by employing

$$t=(\nu\tau)/V_\infty^2,\ \ y=(\nu\eta)/V_\infty,\ \ u=V_\infty F(\tau,\eta),\ \ u_p=V_\infty F_p(\tau,\eta),\ \ v_p=V_\infty G_p(\tau,\eta)$$
$$P=\rho V_\infty^2 H(\tau,\eta),\ \ \rho_p=\rho_{p\infty}Q_p(\tau,\eta),\ \ \nu=V_\infty^{(m-1)/m}k^{1/m} \qquad (2)$$

where V_∞ and $\rho_{p\infty}$ are the respective free-stream velocity and particle density. It should be noted that when $m=1$ (Newtonian fluid) then $k=\nu$ (fluid-phase kinematic viscosity), and when $n=1$ (Newtonian particle phase) then $k_p=\nu_p$ (particle-phase kinematic viscosity). Substituting Equations (2) into Equations (1) and rearranging yield

$$\partial_\tau Q_p + \partial_\eta(Q_p G_p) = 0, \quad \partial_\eta H - \kappa\alpha(\delta\partial_\eta Q_p + r_v(Q_p - 1)) = 0 \tag{3a,b}$$

$$\partial_\tau F - \partial_\eta((\partial_\eta F)^m) - r_v \partial_\eta F + \kappa\alpha Q_p(F - F_p) = 0 \tag{3c}$$

$$Q_p \partial_\tau F_p - 2^{(n-1)/2}\beta\partial_\eta(Q_p \partial_\eta F_p(1/2(\partial_\eta F_p)^2 + (\partial_\eta G_p)^2)^{(n-1)/2}) + Q_p G_p \partial_\eta F_p - \alpha Q_p(F - F_p) = 0 \tag{3d}$$

$$Q_p \partial_\tau G_p - 2^{(n+1)/2}\beta\partial_\eta(Q_p \partial_\eta G_p(1/2(\partial_\eta F_p)^2 + (\partial_\eta G_p)^2)^{(n-1)/2}) + Q_p G_p \partial_\eta G_p + \alpha Q_p(r_v + G_p) + \alpha\delta\partial_\eta Q_p = 0 \tag{3e}$$

where $r_v = V_w/V_\infty$, $\kappa = \rho_{p\infty}/\rho$, $\beta = (k_p V_\infty^{2(n-1)})/\nu^n$, $\alpha = (N\nu)/V_\infty^2$ and $\delta = D/\nu$ are the suction parameter, the particle loading, the viscosity ratio, the inverse Stokes number, and the inverse Schmidt's number, respectively.

The initial and boundary conditions employed to solve Equations (3) are

$$\begin{gathered} F(0,\eta) = 1.0, \; F_p(0,\eta) = 1.0, \; G_p(0,\eta) = -r_v, \; H(0,\eta) = 0, \; Q_p(0,\eta) = 1.0 \\ F(\tau,0) = 0, \; F_p(\tau,0) = \omega(\partial_\eta F_p(\tau,0))^n, \; H(\tau,0) = 0, \; G_p(\tau,0) = G_{p0} \\ F(\tau,\infty) = 1.0, \; F_p(\tau,\infty) = 1.0, \; Q_p(\tau,\infty) = 1.0, \; G_p(\tau,\infty) = -r_v \end{gathered} \tag{4}$$

where G_{p0} and ω are constants. It is an experimental fact that particles flowing close to a surface experience a certain amount of wall slip. This is taken into account by using the seventh equation in Equations (4) which is borrowed from rarefied gas dynamics (see, for instance, Soo [10]). In general, ω will depend on the other parameters of the problem. However, no attempt was made herein to relate ω to the internal properties of the suspension.

The displacement thicknesses and the skin-friction coefficients for both the fluid and particle phases are of special interest and significance for this type of flow. These can, respectively, be defined in dimensionless form as

$$\Delta(\tau) = \int_0^\infty (1 - F)\,d\eta, \quad \Delta_p(\tau) = \int_0^\infty (1 - F_p)\,d\eta, \quad C(\tau) = (\partial_\eta F(\tau,0))^m, \quad C_p(\tau) = \beta\kappa(\partial_\eta F_p(\tau,0))^n \tag{5}$$

Results and Discussion

The initial-value problem represented by Equations (3) and (4) does not posses a closed-form solution. For this reason, a numerical method based on the finite-difference methodology similar to that discussed by Blottner [11] and Patankar [12] is chosen for the solution of the problem under consideration. Equations (3a) and (3b) were solved for Q_p and H, respectively. Equations (3c-e) were solved for F, F_p, and G_p, respectively. All first-order time derivatives are replaced by a two-point backward difference formulas. Equations (3c-e) are discretized using three-point central difference quotients while Equations (3a) and (3b) are solved by the trapezoidal rule. The problem is solved line by line starting at the initial motion of suspension and ending at the steady-state conditions at large time. Linear tri-diagonal algebraic equations were solved (with iteration being employed to deal with the nonlinear nature of the governing equations) by the Thomas' algorithm at each time step as discussed by Carnahan, et al. [13]. Constant time step sizes and variable space step sizes are employed. A 1001 time lines are used with a step size of 0.01 while the η coordinate is represented by 205 meshes. The initial space step size utilized is 0.001 with a growth factor of 1.03. These values were chosen after many numerical tests performed to insure grid independence. A convergence criterion based on the percent difference between the current and the previous iterations is used and the solution was assumed converged when this reached 1%. It should be mentioned that due to the highly nonlinear nature of the governing equations, caution must be exercised in obtaining the numerical results. No convergence difficulties were encountered throughout this work. A large number of computations were performed and many results were produced. Due to page limitations, only a representative set of graphical results for G_{p0}=-2.0 will be presented in figures 1 through 6 to illustrate the effects of the particle loading κ and the fluid-phase behavior coefficient m on the solutions.

Figures 1 and 2 illustrate the temporal development of the fluid-phase displacement thickness Δ and the particle-phase displacement thickness Δ_p for various values of the particle loading κ, respectively. Initially, the velocities of both phases are assumed constant and, therefore, Δ and Δ_p are correspondingly zero. As time progresses, the displacement thicknesses of both phases begin to grow and continue to do that until steady-state conditions are attained where all dependent variables as well as Δ and Δ_p no longer vary with time. This is clearly evident from figures 1 and 2. For κ=0 the carrier fluid motion is independent of the presence of particles. This is called the dilute or clean fluid limit. Increases in the particle loading have a tendency to confine viscous effects to an increasingly small region in the vicinity of the plate surface. This is reflected in the decreases observed in both Δ and Δ_p as κ increases.

Figures 3 and 4 present the time history of the fluid-phase skin-friction coefficient C and the particle-phase skin-friction coefficient C_p for different values of κ, respectively. Initially, both C and C_p are large and their values decay as time increases to reach steady-state conditions. As mentioned previously, increases in particle loading reduce the region near the plate in which viscosity is important. This, in turn, causes the slope of the fluid-phase velocity profile at the wall to increase. This is reflected in the increases in C caused by increasing κ shown in figure 3. Also, since C_p is defined as directly proportional to κ, increases in κ tend to increase C_p as evident from figure 4.

Figures 5 and 6 depict the effects of the fluid-phase behavior coefficient m on Δ and Δ_p, respectively. As m increases, both the fluid- and particle-phase velocities tend to approach the free-stream conditions faster causing a reduction in the values of Δ and Δ_p as clearly evident from figures 5 and 6. Results for the skin-friction coefficients of both phases were also obtained (but not presented herein for brevity) and found to be slightly dependent on m.

It should be mentioned that the steady-state results of the present work are in excellent agreement with those reported previously by Chamkha [9]. Also, favorable comparisons with the transient and steady-state special cases of Newtonian suspension ($m=1$ and $n=1$) reported by Chamkha and Peddieson [7,8]. These comparisons lend confidence in the correctness of the numerical results. Since experimental data on the present problem are lacking at present, no comparisons with such data were performed.

Conclusion

The problem of transient, laminar non-Newtonian flow of a particulate suspension exhibiting non-uniform particle-phase density distribution over an infinite porous flat plate is solved numerically by the finite-difference method. Both phases are assumed to have power-law stress-strain rate relationships. A representative set of graphical results was selected, presented and discussed to show the effects of the particle loading and the fluid-phase behavior coefficient on the flow properties. It was found that increasing the particle loading caused the displacement thicknesses of both phases to decrease and their skin-friction coefficients to increase. Also, as the fluid-phase behavior coefficient increased from pseudo-plastic type behavior ($m<1$) to dilatant type behavior ($m>1$), the displacement thicknesses of both phases decreased and the skin-friction coefficients changed slightly. Excellent agreement between the numerical results reported herein and published Newtonian results was achieved. It is hoped that the present results will be of value in some applications of filtration and serve in validating numerical routines.

References

[1] S. L. Soo, Multiphase Fluid Dynamics, Science Press, (1990).

[2] F. E. Marble, Dynamics of Dusty Gases, Annual Review of Fluid Mechanics, **2** (1970), 397-446.

[3] J. Peddieson, On Continuum Description of Solid-Fluid Suspensions, Developments in Theoretical and Applied Mechanics, **7** (1974), 355-368.

[4] J. D. Ramshaw, Brownian Motion in a Flowing Fluid, Physics of Fluids, **22** (1979), 1595-1601.

[5] A. G. Fredrickson, Principles and Applications of Rheology, Prentice Hall, Inc., (1964).

[6] J. N. Kapur, Flows of Power-Law Fluids Past a Flat Plate with Uniform Suction and Between Two Parallel Plates with Uniform Suction and Injection, Journal of the Physical Society of Japan, **18** (1963), 578-582.

[7] A. J. Chamkha, and J. Peddieson, The Asymptotic Suction Profile For a Particulate Suspension, Developments in Theoretical and Applied Mechanics, **15** (1990), 43-50.

[8] A. J. Chamkha, and J. Peddieson, Unsteady Dusty-Gas Flow With Suction, Engineering Science Preprint-27, (1990).

[9] A. J. Chamkha, Flow of Non-Newtonian Particulate Suspension With a Compressible Particle Phase, Mechanics Research Communications, **21**, (1994), 645-654.

[10] S. L. Soo, Pipe Flow of Suspensions, Applied Scientific Research, **21** (1969), 68-84.

[11] F. G. Blottner, Finite Difference Methods of Solutions of the Boundary-Layer Equations, AIAA Journal, **8** (1970), 193-205.

[12] S. V. Patankar, Numerical Heat Transfer and Fluid Flow, McGraw-Hill New York (1980).

[13] B. Carnahan, et al., Applied Numerical Methods, Chapter 7, (1969).

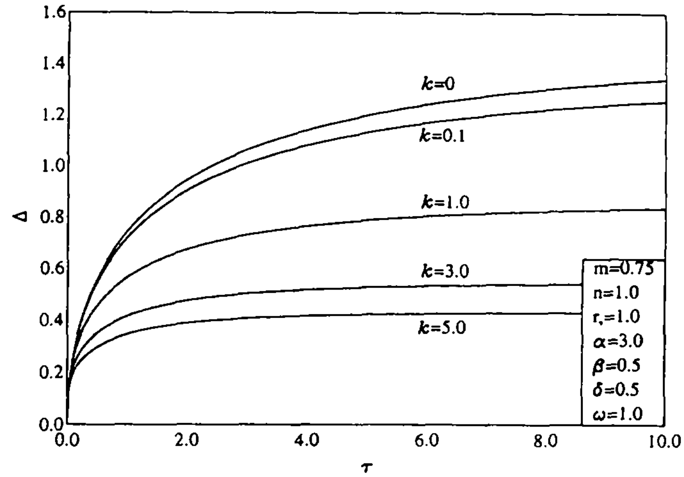

Figure 1. Effects of k on the Fluid-Phase Displacement Thickness

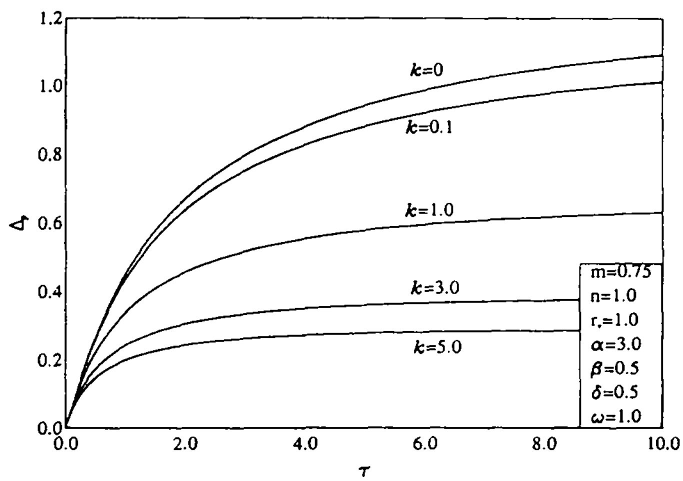

Figure 2. Effects of k on the Particle-Phase Displacement Thickness

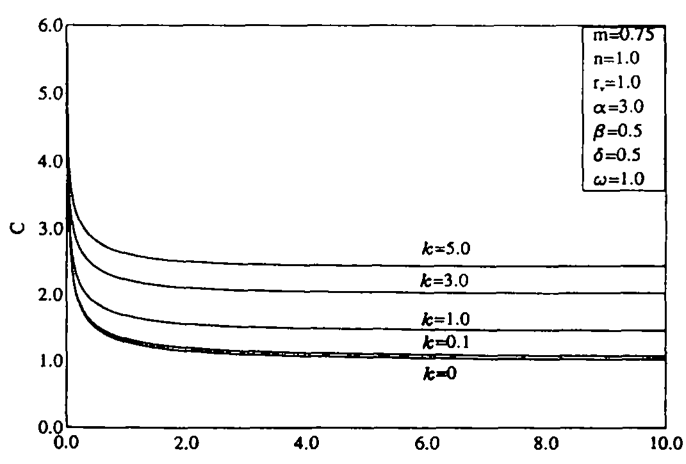

Figure 3. Effects of k on the Fluid-Phase Skin-Friction Coefficient

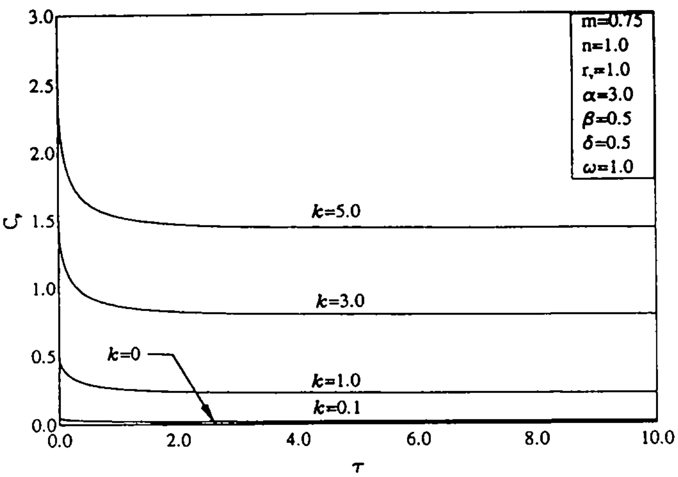

Figure 4. Effects of k on the Particle-Phase Skin-Friction Coefficient

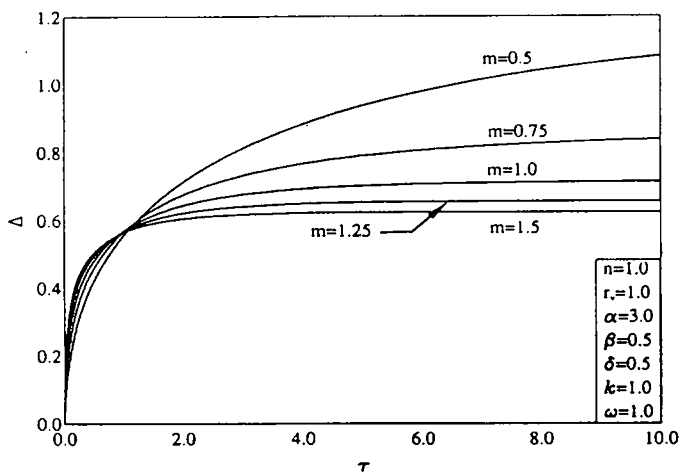

Figure 5. Effects of m on the Fluid-Phase Displacement Thickness

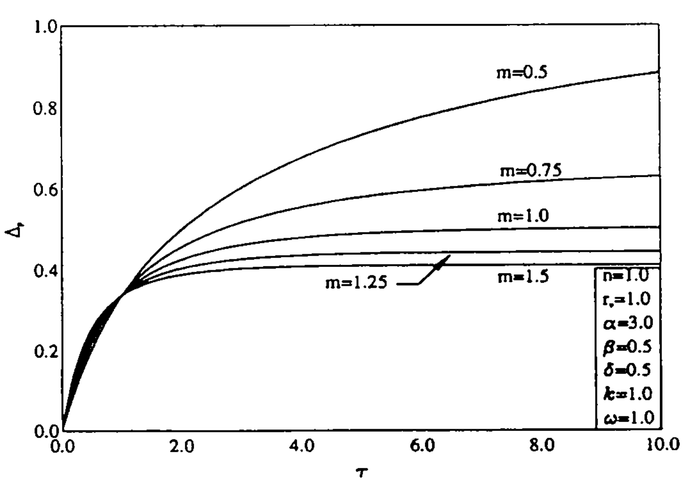

Figure 6. Effects of m on the Particle-Phase Displacement Thickness